Toxicology 470 (2022) 153153

Contents lists available at ScienceDirect

Toxicology

journal homepage: www.elsevier.com/locate/toxicol

Cadmium acute exposure induces metabolic and transcriptomic perturbations in human mature adipocytes

Marie Gasser [a,b], Sébastien Lenglet [a], Nasim Bararpour [a,b,1], Tatjana Sajic [a,b], Kim Wiskott [c], Marc Augsburger [a], Tony Fracasso [c], Federica Gilardi [a,b], Aurélien Thomas [a,b,*]

[a] Unit of Forensic Toxicology and Chemistry, CURML, Lausanne and Geneva University Hospitals, Lausanne, Geneva, Switzerland
[b] Faculty Unit of Toxicology, CURML, Faculty of Biology and Medicine, University of Lausanne, Lausanne, Switzerland
[c] Unit of Forensic Pathology, CURML, Lausanne and Geneva University Hospitals, Lausanne, Geneva, Switzerland

ARTICLE INFO

Handling Editor: Dr. Thomas Knudsen

Keywords:
Cadmium
Human adipocytes
Cellular homeostasis
Metallothioneins
SLC transporters
Adipose tissue concentrations

ABSTRACT

Obesity is considered as a major public health concern with strong economic and social burdens. Exposure to pollutants such as heavy metals can contribute to the development of obesity and its associated metabolic disorders, including type 2 diabetes and cardiovascular diseases. Adipose tissue is an endocrine and paracrine organ that plays a key role in the development of these diseases and is one of the main target of heavy metal accumulation. In this study, we determined by inductively coupled plasma mass spectrometry cadmium concentrations in human subcutaneous and visceral adipose tissues, ranging between 2.5 nM and 2.5 μM. We found a positive correlation between cadmium levels and age, sex and smoking status and a negative correlation between cadmium and body mass index. Based on cadmium adipose tissue concentrations found in humans, we investigated the effects of cadmium exposure, at concentrations between 1 nM and 10 μM, on adipose-derived human mesenchymal stem cells differentiated into mature adipocytes in vitro. Transcriptomic analysis highlighted that such exposure altered the expression of genes involved in trace element homeostasis and heavy metal detoxification, such as Solute Carrier Family transporters and metallothioneins. This effect correlated with zinc level alteration in cells and cellular media. Interestingly, dysregulation of zinc homeostasis and transporters has been particularly associated with the development of obesity and type 2 diabetes. Moreover, we found that cadmium exposure induces the pro-inflammatory state of the adipocytes by enhancing the expression of genes such as IL-6, IL-1B and CCL2, cytokines also induced in obesity. Finally, cadmium modulates various adipocyte functions such as the insulin response signaling pathway and lipid homeostasis. Collectively, our data identified some of the cellular mechanisms by which cadmium alters adipocyte functions, thus highlighting new facets of its potential contribution to the progression of metabolic disorders.

1. Introduction

In the last decades, obesity has become a major public health concern with the high increase of its rate since the seventies (OECD, 2019) and a strong economic and social impact for the health authorities. Obesity is characterized by an enlargement of the adipose tissue, mainly as an unhealthy expansion (Longo et al., 2019), associated with the development of inflammation, accumulation of immune and hypertrophic adipocyte cells and insulin sensitivity decrease. These dysregulations can finally lead to metabolic complications such as type 2 diabetes (T2D) or cardiovascular diseases. In addition to increased high caloric food intake, decrease of physical activity and genetic predispositions,

Abbreviations: AD-hMSC, Adipose-Derived human Mesenchymal Stem Cell; ADIPOQ, Adiponectin; CCL2, C-C Motif Chemokine Ligand 2; Cd, Cadmium; $CdCl_2$, Cadmium Chloride; GLUT4, Glucose Transporter Type 4; IC50, Inhibitory Concentration 50; ICP-MS, Inductively Coupled Plasma Mass Spectrometry; IRS2, Insulin Receptor Substrate 2; LEP, Leptin; LIMMA, Linear Model for Microarray Data; MT, Metallothionein; MT1A, Metallothionein 1A; MT1B, Metallothionein 1B; MT2A, Metallothionein 2A; PCK1, Phosphoenolpyruvate Carboxykinase 1; PPARG, Peroxisome Proliferator Activated Receptor Gamma; RPS13, Ribosomal Protein S13; SAT, Subcutaneous Adipose Tissue; SLC, Solute Carrier Family; SLC30A1, Solute Carrier Family 30 Member 1; SLC39A8, Solute Carrier Family 39 Member 8; UPLC-HRMS, Ultrahigh Pressure Liquid Chromatography coupled to High Resolution Mass Spectrometry; VAT, Visceral Adipose Tissue; Zn, Zinc.

* Corresponding author at: Unit of Forensic Toxicology and Chemistry, CURML, Lausanne and Geneva University Hospitals, Lausanne, Geneva, Switzerland.
E-mail address: aurelien.thomas@chuv.ch (A. Thomas).
[1] Present address: Department of Genetics, Stanford School of Medicine, Stanford, CA 94305, USA.

https://doi.org/10.1016/j.tox.2022.153153
Received 4 October 2021; Received in revised form 15 February 2022; Accepted 9 March 2022
Available online 14 March 2022

exposure to various pollutants might contribute to obesity and its associated metabolic disorders. These pollutants, named obesogens, can disrupt adipocyte functions by promoting adiposity and adipogenesis (Janesick and Blumberg, 2011, 2016). In particular, the increased risk of obesity and the development of metabolic diseases such as T2D are significantly higher in cases of chronic exposure to heavy metals such as cadmium, arsenic and mercury (Afridi et al., 2008; Chen et al., 2009). These heavy metals mainly accumulate in liver and kidneys (Kayaalti et al., 2010; Park and Zheng, 2012; Yi et al., 2020), but also in adipose tissue (Freire et al., 2020), and several studies have determined the biological concentrations of these compounds in different samples, such as blood, urine and hair (Coelho et al., 2014; Heitland and Koster, 2006; Yedomon et al., 2017).

Cadmium (Cd) is classified as a group I carcinogen by the International Agency for Research on Cancer (IARC). Some of the predominant routes of Cd exposure are through cigarettes (Milnerowicz et al., 2015), food contamination and industrial pollution (Genchi et al., 2020; Satarug et al., 2010). Cd concentration is significantly higher in the blood and urine of smokers compared to non-smokers (Bochud et al., 2018; Heitland and Koster, 2006). The living environment and profession also contribute to Cd accumulation in the body and higher blood concentrations are observed in blue- than in white-collar worker blood (Coelho et al., 2014; Yedomon et al., 2017). Elderly patients have higher blood Cd concentrations due to an effect of accumulation during life and food intake. As mentioned above, Cd exposure can be associated with an increased risk of obesity and the development of T2D and prediabetes (Wallia et al., 2014). Diabetic patients have higher blood Cd concentrations compared to controls, independently of their smoking habits (Afridi et al., 2008; Chen et al., 2009). Workers exposed to Cd have increased blood glucose level and decreased serum insulin levels (Chen et al., 2009). Cd toxicity is also associated with the risk of development of cardiovascular diseases (Barregard et al., 2016; Tellez-Plaza et al., 2012) and chronic kidney disease (Hellstrom et al., 2001). Strong accumulation of Cd in kidneys and human urine samples show positive associations with increased steroid hormone metabolite levels (corticosteroids such as glucocorticoids and mineralocorticoids) (Bochud et al., 2018). Moreover, urinary concentrations of Cd are positively correlated with higher body mass index (BMI) (Bochud et al., 2018) and are associated with the induction of adipocyte differentiation, increased adiposity and insulin resistance (Akalestou et al., 2020). Because of this obesogen potential of Cd and its accumulation in body tissues, recent studies quantified Cd concentrations in adipose tissues of living and dead patients (Echeverria et al., 2019; Egger et al., 2019).

To understand and characterize the molecular and cellular perturbations induced by Cd in human adipose tissue at environmentally relevant concentrations, we first quantified concentrations of Cd and other trace elements in human visceral and subcutaneous adipose tissue samples collected at forensic autopsy in our center. Based on this, we established a range of concentrations, between 1 nM and 10 μM of Cd, for in vitro experiments on a human cellular model of adipocytes, adipose-derived human mesenchymal stem cells (AD-hMSCs). AD-hMSCs are directly derived from the stromal vascular fraction of human adipose tissue and are able to differentiate into mature adipocytes in vitro. They have proven to be a good model for the study of adipose tissue cellular physiology (Dufau et al., 2021) and they present many experimental advantages such as a high expansion capacity, the ability to be passaged a high number of time and cryopreserved, and multipotency. We assessed Cd cytotoxicity on AD-hMSCs after 48 h of exposure and evaluated its impact on the cellular function, transcriptome, metabolome, and metallome.

Our results demonstrate that Cd acute exposure induced metabolic and transcriptomic perturbations in human adipocytes by modulating the levels of many transporters in cells, zinc (Zn) homeostasis and various adipocyte functions.

2. Materials and methods

2.1. Cell culture and treatment

The adipose-derived human mesenchymal stem cells (FC-0034) were purchased at Lifeline Cell Technology (Frederick, MD, USA). AD-hMSCs are derived from adipose tissue and isolated from adult lipoaspirate. Cells are selected by the manufacturer via flow cytometry to ensure the expression of multiple mesenchymal stem cell markers and can be differentiated into adipocytes. Cells were expanded at 37 °C and 5% CO_2 in MesenPro RS Basal Medium supplemented with MesenPro RS Growth Supplement (Gibco, Thermo Fisher Scientific, Waltham, MA, USA) and 2 mM GlutaMAX-I (Gibco) following manufacturer instructions. MesenPro RS Medium is a reduced serum (2%) medium and is specially formulated for the growth and maintenance of human mesenchymal stem cell cultures. When they reached 80% confluency, cells are splitted and seeded into 6-, 12- or 24-well plates at 9×10^3 cells/cm^2 with MesenPro RS Medium until they reached confluency. Cells were induced to differentiate into adipocytes in StemPro Adipogenesis Differentiation Basal Medium supplemented with StemPro Adipogenesis Supplement (Gibco), following manufacturer instructions. The StemPro Adipogenesis Differentiation medium is especially formulated for the adipogenic differentiation of human mesenchymal stem cells and contains all the reagents required to induce AD-hMSCs to differentiate into adipocytes. StemPro medium contains high glucose, GlutaMAX-I, calcium, sodium phosphate, standard serum level, sodium bicarbonate, sodium pyruvate and adipogenesis supplements. Cells were refed every 3 – 4 days. After two weeks of differentiation, adipocytes were incubated with cadmium chloride ($CdCl_2$, Sigma-Aldrich, Saint-Louis, MO, USA) solutions for 48 h at 37 °C and 5% CO_2. Concentrations of $CdCl_2$ between 1 nM and 0.5 M were used in this study. $CdCl_2$ powder was dissolved in ultra-pure water (Milli-Q) and diluted in MesenPro RS Basal Medium supplemented with 2 mM Glutamax-I.

2.2. Trace element quantification in human adipose tissues and cells

Human adipose tissue samples from 100 donors were collected at autopsy at the CURML (University Center of Legal Medicine, Switzerland). The project was authorized by the Research Ethics Committee of Vaud, Switzerland (CER n°2019–01877). Samples were anonymized and stored at − 20 °C before mineralization and analysis. In our study, omentum visceral and abdominal subcutaneous depots were used to quantify trace elements. Adipose tissue samples were mineralized in HNO_3 65% by heating for 1 h at 80 °C.

AD-hMSCs were differentiated into adipocytes in 6-well plates and treated with $CdCl_2$ (1 nM – 10 μM) in quintuplicates for 48 h. After the treatment, cell media were transferred into 2 mL Eppendorf tubes for further preparation. Cells were washed with phosphate-buffer saline (PBS, Gibco) and 320 μL of 65% nitric acid (HNO_3) were added to each well to extract cell lysates.

Trace element concentrations were measured in cells and tissues by inductively coupled plasma mass spectrometry (ICP-MS; 7800 Series; Agilent, Palo Alto, Santa Clara, CA, USA) as described previously (Jafari et al., 2018) for elementary quantification: aluminum, antimony, arsenic, bismuth, cadmium, chromium, cobalt, copper, lead, lithium, manganese, molybdenum, nickel, selenium, zinc. 300 μL of cell or tissue sample were diluted with 2.7 mL of HNO_3 0.1% solution containing 10 ng/mL Rhodium and 10 ng/mL Indium as internal standards. In addition, each analytical batch of study samples was processed with laboratory controls, including method blanks and standard reference materials to continuously monitor method performance.

2.3. Cell viability assay

AD-hMSCs were differentiated into adipocytes in 24-well plates and treated with $CdCl_2$ (1 nM – 0.5 M) in duplicate (for Cd concentrations

between 1 nM and 100 nM and between 0.05 and 0.5 M), in triplicate (for Cd concentrations between 500 nM and 0.01 M) and quadruplicate (for controls) for 48 h. Cell viability after Cd treatment was assessed using the Cell Proliferation Kit I (MTT) (Roche, Basel, Switzerland), following manufacturer instructions. The plates were incubated at 37 °C and 5% CO_2 for 20 min with the MTT reaction mix and dimethyl sulfoxide (DMSO, Sigma-Aldrich) was used to extract the coloration. The absorbance was measured in duplicate at 540 nm in a 96-well microplate with the Infinite M Nano Reader (Tecan, Männedorf, Switzerland). The viability rate was calculated using non-linear regression to fit the Hill function in GraphPad Prism version 8.0.0 for Windows (GraphPad Software, San Diego, CA, USA, www.graphpad.com). The presented results are the mean of two independent experiments.

2.4. Western Blot

AD-hMSCs were differentiated into adipocytes in 6-well plates and treated with CdCl2 (1 μM and 10 μM, N = 2) for 48 h in complete differentiation medium. Cells were serum-starved overnight the 16 last hours of cadmium treatment. Proteins were extracted on ice with 200 μL of M-PER Mammalian Protein Extraction Reagent (Thermo Fisher Scientific) supplemented with Halt Protease/Phosphatase Inhibitor Cocktail (100X, Thermo Fisher Scientific). Proteins were transferred into Eppendorf tubes and let in ice for 5 min. Tubes were then centrifuged for 10 min at 13'300 g and 4 °C. Supernatants were transferred into new tubes and sample protein concentrations were quantified with the Pierce BCA Protein Assay Kit (Thermo Fisher Scientific) following manufacturer instructions. 11.5 μg of proteins per sample were used for Western-blots.

Protein samples were analyzed by SDS/PAGE with standard procedures (gradient 12.5% acrylamide) and electroblotted onto Protran BA85, 0.45 μm pore size nitrocellulose membrane (Whatman, Maidstone, United Kingdom). After 1 h in blocking buffer (Tris-buffered saline (TBS) - Tween 20 0.1% (TBS-T 0.1%) with 5% fat free dry milk), membranes were blotted overnight at 4 °C with phospho-Akt (Ser473) Antibody (9271, dilution 1:1'000, Cell Signaling Technology) or Akt Antibody (9272, dilution 1:1'000, Cell Signaling Technology) diluted in blocking buffer. After three washing steps with TBS-T 0.1%, membranes were incubated for 1 h at room temperature with ECL Anti-Rabbit IgG conjugated with horseradish peroxidase diluted 1:30'000 and 1:20'000 in blocking buffer respectively for Akt and phospho-Akt. After three additional washing steps with TBS-T 0.1%, protein bands were detected by chemiluminescence using ECL Select Western Blotting Detection Reagent (Cytiva, Amersham, United Kingdom). Mild stripping was used on each membrane for restaining with GAPDH antibody. The stripping buffer was 15% glycine, 1% Sodium Dodecyl Sulfate (SDS) and 10% Tween 20 in distilled water. pH was adjusted to 2.2. Membranes were incubated two times with stripping buffer for 10 min, then washed with PBS two times for 10 min and with TBS-T 0.1% two times for 5 min. Membranes were then ready for blocking and the end of the experiment as described previously. Membranes were blotted for one hour at room temperature with Rabbit mAb against GAPDH (14C10, dilution 1:1'000, Cell Signaling Technology) diluted in blocking buffer and incubated for 1 h at room temperature with ECL Anti-Rabbit IgG conjugated with horseradish peroxidase diluted 1:30'000. Images were processed using ImageJ software (Schneider et al., 2012).

2.5. Triglyceride content

AD-hMSCs were differentiated into adipocytes in 6-well plates and treated with $CdCl_2$ concentrations (1 μM and 10 μM) for 48 h. Eight replicates per conditions were used and triglyceride content was measured with the EnzyChromTM Triglyceride Assay Kit (BioAssay Systems, Cat# ETGA-200, Hayward, CA, USA) following the manufacturer instructions.

2.6. Transcriptomic study

AD-hMSCs were differentiated into adipocytes in 12-well plates and treated with 1 μM of $CdCl_2$ for 48 h (N = 3). Total RNA was isolated from Cd-exposed cells using the Direct-zol RNA MiniPrep Kit (Zymo Research, Lucerna-Chem, Luzern, Switzerland) following manufacturer protocol. RNA concentrations were quantified using the Qubit Fluorometer (Invitrogen, Life Technologies, Carlsbad, CA, USA) following manufacturer instructions. 100 ng of total RNA were used as input for the preparation of labeled double strand cDNA using the GeneChip Pico reagent kit (Thermo Fisher Scientific). Targets were hybridized on Human Clariom S arrays according to recommendations. Linear Models for Microarray data (LIMMA) using R software were applied to compare control samples versus Cd-treated samples (Ritchie et al., 2015). LIMMA is a core component of R and a Bioconductor package, an open-source software development project in statistical genomics, specifically designed for the analysis of gene expression variations between treatment conditions. The principle is based on linear models fitted to each gene of the dataset, which is analyzed as an entire whole of observations, by leveraging the highly parallel nature of genomic data to borrow strength between the gene-wise models. Differences were considered significant if the fold-change was > 1.5 and the adjusted p-value (adj. p-value) was < 0.05. For heatmaps, data were clustered in R by Ward's clustering with the Euclidean distance.

2.7. RNA Extraction and quantitative PCR

In order to validate the micro-array data on a larger range of concentrations and in independent experiments, we performed RT-qPCR at five Cd concentrations. AD-hMSCs were differentiated into adipocytes in 12-well plates and treated with $CdCl_2$ (1 nM – 10 μM) for 48 h (N = 11 for controls, N = 5 for Cd concentrations). The experiment was performed at least twice in cells coming from different donors. Total RNA was isolated, extracted and quantified as described in Section 2.6. cDNA was synthesized using 140 ng of total RNA with the Impro-II Reverse Transcription System kit (Promega, Madison, WI, USA) following manufacturer instructions. For real-time quantitative PCR (RT-qPCR), the target genes were amplified with the KAPA PROBE FAST qPCR Master Mix (2X) Kit (KapaBiosystems, Sigma-Aldrich). The qPCR program was 50 °C for 2 min, 95 °C for 3 min, followed by 46 cycles of 95 °C for 15 s and 60 °C for 30 s. IRS2 gene was amplified with the KAPA SYBR FAST qPCR Master Mix (2X) Kit (KapaBiosystems). The qPCR program was 10 min at 95 °C followed by 40 cycles of 95 °C for 10 s and 62 °C for 20 s, associated with a melt curve stage of 15 s at 95 °C, one minute at 60 °C and then increases of 0.3 °C every 15 s to reach 95 °C. The selected primer sets used in this study are summarized in Table 1. Results were normalized to Ribosomal Protein S13 (RPS13) as a housekeeping gene and relative expression was calculated with the $2^{-\Delta\Delta Ct}$ method.

2.8. Metabolomic study

2.8.1. Metabolites extraction

AD-hMSCs were differentiated into adipocytes in 6-well plates and treated with 1 μM of $CdCl_2$ for 48 h. Six replicates were used for the study. Cells were washed with PBS and immediately putted on dry ice. 1.5 mL of mix solvent MeOH/EtOH/H_2O 2:2:1 containing 500 ng/mL of internal standards, hydrocodone-d6 and phenobarbital-d5, were added into each well and the plates were incubated at − 80 °C for 20 min. The cells were scraped and transferred into 2 mL Eppendorf tubes on dry ice. The tubes were agitated during 5 min with metallic beads and centrifuged for 5 min at 4 °C and 14'000 rpm to pellet cellular debris. The metabolite-containing supernatants were transferred into new Eppendorf tubes on dry ice and evaporated for 4 h with a CentriVap Concentrator (Labconco, Kansas City, MO, USA).

Table 1
Forward and reverse primers and probes used for RT-qPCR.

Gene	Primer Sequence Forward	Primer Sequence Reverse	Probe	Accession Number
RPS13	CGTCCCCACTTGGTTGAAG	TTGTGCAACACCATGTGAATC	TGACATCTGACGACGTGAAGGAGCA	NM_005953.4
MT2A	CAACCTGTCCCGACTCTAG	GCAGCTTTTCTTGCAGGAG	TTCAGCTCGCCATGGATCCCAA	NM_005947.2
MT1B	CCCTGACTTCTCATATCTTGCC	GGAGGTACATTTGCACTCTTTG	AGGAACTCCAGGCTTGTCTTGGC	NM_005946.2
MT1A	CACTGGCTCCTGCAAATG	ACTTCTCTGATGCCCCTTTG	ATGAGCTGTGCCAAGTGTGCC	NM_001017.3
PPARG	TCTCATAATGCCATCAGGTTTG	ATCTCCGCCAACAGCTTCT	CGGATGCCACAGGCCGAGAA	NM_005037.6
CCL2	AGCAAGTGTCCCAAAGAAGC	TGAACCCACTTCTGCTTGG	ATCTTCAAGACCATTGTGGCCAAGG	NM_002982.4
LEP	CACACGCAGTCAGTCTCCTC	TCTTGGATAAGGTCAGGATGG	CGGTTTGGACTTCATTCCTGGGCT	NM_000230.3
PCK1	GTTTGACGCACAAGGTCATTT	TGTGTTCTTCTGCATGGTCTTG	TTTCGGTGTCGCTCCTGGGACTT	NM_002591.4
ADIPOQ	CATACCAGAGGAGACGGGATT	GCATCCTGAGCCCTGATGT	CATGTTGTCCAGGCTGGTCTGAAACTC	NM_001177800.2
SLC39A8	GCTACCCAAATAACCAGCTCC	CACTGACAGGAATCCATATCCC	TCGGCCCAAGCACAAAACAAGAC	NM_001135147.1
SLC30A1	ATACCAGCAACTCCAACGG	TGTTAAGTTGTCCAGCCCTATC	CGCAGACCCAGAAAACCCCAGAA	NM_021194.3
IL6	CAATGAGGAGACTTGCCTGGT	CAGGAACTGGATCAGGACTTTT	AATCATCACTGGTCTTTTGGAGTTTGAGGT	NM_000600.5
IL1B	ATCTTCATTGCTCAAGTGTCTGAA	CTGGAAGGAGCACTTCATCTG	CAGAAGTACCTGAGCTCGCCAGTGAAA	NM_000576.3
GLUT4	TCGGTTCTTTCATCTTGGCC	AGAACACAGCAAGGACCAG	CGGGCTTCCAACAGATAGGCTCC	NM_001042.3
IRS2	ACTTCTTGTCCCACCACTTG	TGACATCCTGGTGATAAAGCC	–	NM_003749.3

2.8.2. Sample preparation

The pellets were resuspended in 100 μL of 10% MeOH and centrifuged for 5 min at 8 °C and 14'000 rpm. The resulting supernatant was divided into two fractions of 40 μL and were transferred into two glass vials for injection in positive and negative modes. Quality control (QCs) samples were a pooled matrix sample generated by combining 10 μL of each experimental sample. QCs were injected 9 times across the batches.

2.8.3. Untargeted mass spectrometry analysis

Untargeted mass spectrometry analysis was performed using ultra-high performance liquid chromatography coupled to high-resolution mass spectrometry (UPLC-HRMS). A Thermo Scientific Ultimate 3000 LC system coupled to a Q Exactive Plus system interfaced with a heated electrospray ionization (HESI-II) was used for the study. Positive and negative ion mode analyses used mobile phase consisting of 0.1% formic acid in water (A) and 0.1% formic acid in methanol (B), respectively. The sample injection volume was 3 μL and separation was made using a C18 column (Phenomenex Kinetex, C18 – 100 ×2.1 mm, 2.6 μm) held at 40 °C. Mobile phase B was ramped linearly from 2% to 98% over 6 min, reached 100% at the 9th minute and brought back to 2% for a 4 min re-equilibration. The total analysis run was 13 min with a flow of 300 μL/min. The mass analyzer was tuned and calibrated for mass resolution and mass accuracy and the full scan range covered 70–1'000 *m/z*. The ionization spray voltage was set to 3.20 and 2.90 kV in positive and negative mode respectively, the sheath gas flowrate to 40 and 10, and the auxiliary gas flowrate to 10 only in positive mode (both gas flowrate in arbitrary units). The acquisition software was Xcalibur 3.1.66.10.

2.8.4. Data analysis

Raw UPLC-HRMS data were converted to mzXML format using ProteoWizard (Chambers et al., 2012) to be processed by XCMS online software (The Scripps Research Institute, San Diego, CA, USA) for peak detection and chromatogram alignment. Missing data were estimated with the dbnorm R package, using emvd function (Bararpour et al., 2021). Preprocessed data were normalized by the MS Total Useful Signal (MSTUS) normalization method available on the NOREVA online software (Yang et al., 2020). Spearman correlation, as calculated using R software, was used to compare the 1 μM condition to control to assess the relationship between the two variables, namely metabolites and Cd concentrations. Spearman correlation coefficient allows to determine the strength and the direction of the association between the variables. Differences were considered statistically significant if the p value was < 0.05. Significant metabolites were identified based on their mass to charge ratio and retention time using the Human Metabolome Database (HMDB). For heatmaps, data were clustered in R by Ward's clustering with the Euclidean distance.

2.9. Pathway over-representation analysis

Over-representation pathway analysis of the transcriptomic and metabolomic data at 1 μM was performed using the Integrated Molecular Pathway Level Analysis (IMPaLA) software (Kamburov et al., 2011) exploiting KEGG, SMPDB, Reactome and Wikipathways databases. For separated analysis, pathways were considered significantly enriched when the q-value was < 0.05. For combined analysis of transcriptomic and metabolomic data, pathways were considered significantly enriched when more than two significantly impacted metabolites and genes were found in the pathway and when the joint q value (the associated adjusted p value for genes and for metabolites) was < 0.05.

2.10. Statistical analysis

Student t-tests were performed using GraphPad Prism version 8.0.0 for Windows to investigate the effect of Cd versus controls (GraphPad Software, San Diego, CA, USA, www.graphpad.com).

To determine relationships among gender, smoking status, BMI, age, post-mortem interval and Cd levels in human subcutaneous and visceral adipose tissues, we performed multiple linear regression analyses using GraphPad Prism. Cd concentrations were expressed as log-transformed variables.

3. Results

3.1. Cadmium concentrations in human adipose tissues

To understand the effects of Cd exposure on human adipose tissue and to determine a range of concentrations for in vitro treatments as close as in vivo exposure, we analyzed Cd concentrations found in 100 anonymized samples of visceral (VAT) and subcutaneous (SAT) adipose tissues, collected at autopsy in our center. Fig. 1A presents the population description. In our cohort, representative of a general population found at forensic autopsy, Cd levels were between 1.4 and 453.8 pg/mg of Cd in VAT, and between 0.4 and 104.8 pg/mg in SAT, corresponding to tissue concentrations between 2.5 nM and 2.5 μM. Interestingly, we found significantly higher concentrations in VAT than in SAT in both sexes and higher Cd concentrations in woman VAT and SAT compared to man depots (Fig. 1B). This last observation was confirmed by the results of the multiple linear regression analyses of the potential predictors of Cd adipose tissue concentrations for subcutaneous and visceral depots, respectively shown in Tables 2 and 3. Moreover, in both adipose tissue depots, we found a strong positive association between Cd concentrations and age and a negative correlation between Cd levels and BMI. The analyses demonstrated that smokers have higher levels of Cd in subcutaneous depots than non-smokers, but not in visceral depots. Finally, we found no correlation between Cd levels in VAT and SAT and post-

(A)

Variables	Men (n = 68)		Women (n = 32)	
Age (years)	50.5 ± 18.8		56.0 ± 20.2	
Smoke, no. (%)	29.0 (42.6)		10.0 (31.3)	
BMI (kg/m2)	26.1 ± 6.3		26.5 ± 8.8	
PMI (hours)	43.2 ± 30.5		41.1 ± 28.0	
Cadmium concentration (pg/mg)	**VAT**	**SAT**	**VAT**	**SAT**
Min	1.4	0.4	7.5	1.6
Max	453.9	104.8	179.1	96.1
Median	16.8	8.1	35.8	11.8
5th percentile	4.4	2.1	7.9	2.5
95th percentile	125.6	51.1	113.0	81.4

(B)

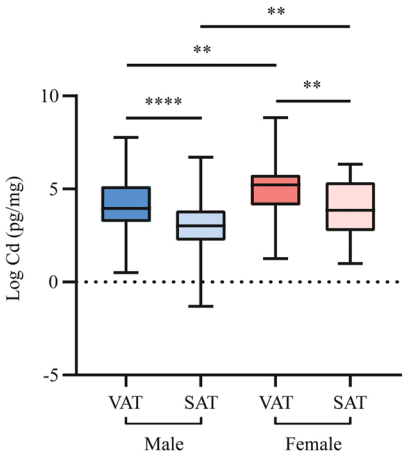

Fig. 1. Cadmium concentrations found in human visceral and subcutaneous adipose tissues. (A) General characteristics of the population and cadmium concentrations found in the adipose tissue depots. Data are given as mean and standard deviation or percent (%). (B) Concentrations of cadmium found in male and female visceral and subcutaneous adipose tissues collected at forensic autopsy, determined by ICP-MS. The box plots indicate the minimum and maximum concentrations at the logarithmic scale. Student t-test was used to analyze the differences between depots and * indicates the significant changes (** $p < 0.01$, **** $p < 0.0001$).

Table 2
Multiple linear regression analysis of log-transformed subcutaneous adipose tissue Cd concentrations (pg/mg).

	Beta	Standard error	p-value
Sex[a]	0.9242	0.3251	0.0058
Smoking status[b]	0.8455	0.2981	0.0059
BMI (kg/m^2)	-0.08522	0.02304	0.0004
Age (years)	0.03137	0.007849	0.0001
PMI (hours)	0.008597	0.005272	0.1077

$R^2 = 0.3493$
Adjusted $R^2 = 0.3146$
[a] Reference category = male
[b] Reference category = non-smoker

mortem interval (PMI).

3.2. Cadmium cytotoxicity and quantification in cells

We first assessed the cytotoxicity of Cd on AD-hMSCs and the half-maximal inhibitory concentration (IC50) of Cd was determined at 19 μM (Fig. 2A). The concentration at 1 μM was the highest level of exposition without significant cytotoxicity, as demonstrated by the reduction of cell viability at concentrations higher than 1 μM (Fig. 2B). The concentrations of Cd in cell lysates were increased in a dose-dependent manner, demonstrating the stable absorption of Cd by cells (Fig. 2C).

Table 3
Multiple linear regression analysis of log-transformed visceral adipose tissue Cd concentrations (pg/mg).

	Beta	Standard error	p-value
Sex[a]	0.8507	0.3161	0.0088
Smoking status[b]	0.5086	0.293	0.0868
BMI (kg/m^2)	-0.08724	0.02284	0.0003
Age (years)	0.03912	0.007559	< 0.0001
PMI (hours)	0.01008	0.005444	0.0689

$R^2 = 0.3493$
Adjusted $R^2 = 0.3146$
[a] Reference category = male
[b] Reference category = non-smoker

Based on these results and on the concentrations experimentally found in human adipose tissues, we determined a range of Cd concentrations from 1 nM to 10 μM, which was used for the subsequent experiments.

3.3. Effect of cadmium on adipocyte function

In adipocytes, glucose uptake in response to insulin is ensured by the glucose transporter type 4 (GLUT4), whose translocation to the cell membrane is mediating a cell signaling cascade including the phosphorylation of Akt (Świderska et al., 2020). In our study, we measured by Western-blots the phosphorylation level of Akt after insulin stimulation and Cd treatment at the two highest concentrations (1 μM and 10 μM), to assess the maximal effect of Cd on this signaling. In controls and at 1 μM of Cd, Akt phosphorylation was increased upon insulin stimulation while, at 10 μM, insulin had no effect on Akt phosphorylation (Fig. 3A). To complete these results, we measured the mRNA expression levels of two genes coding for the Insulin Receptor Substrate 2 (IRS2) and for GLUT4. IRS2 expression significantly decreases from 100 nM in a dose-dependent manner and GLUT4 expression was strongly decreased at 10 μM of Cd (Fig. 3B).

Another major characteristic of adipocytes is their ability to stock lipids in the form of triglycerides and to release them as an energy source. In this study, we investigated the effect of the two highest Cd concentrations on the intracellular triglyceride content. Fig. 3C shows that triglyceride content was slightly decreased in a dose-dependent manner but without significance. We further investigated the effects of Cd treatment on genes involved in adipocyte function and homeostasis such as the Peroxisome Proliferator Activated Receptor Gamma (PPARG), adiponectin (ADIPOQ), leptin (LEP) and the Phosphoenolpyruvate Carboxykinase 1 (PCK1). In mature adipocytes, PPARG regulates the expression of adipocyte genes involved in lipid metabolism, in particular fatty acid biosynthesis and metabolism (Kershaw et al., 2007). The adipokines LEP and ADIPOQ regulate appetite control for the first, insulin sensitivity for the latter and have anti-inflammatory properties in adipose tissue (Fantuzzi, 2005). In parallel, we determined the mRNA level of the C-C Motif Chemokine Ligand 2 (CCL2) and the interleukins 6 (IL6) and 1 beta (IL1B), different markers of inflammation expressed in adipocytes. Gene expression level of LEP was significantly increased at 10 μM of Cd after 48 h of treatment (Fig. 3D). A mild increase of PPARG and CCL2 mRNA levels was observed at 10 nM and 100 nM of Cd and a mild decrease of CCL2, PCK1 and IL6 gene expressions was observed at 10 μM. However, IL1B mRNA level significantly increased at 100 nM and at 10 μM. Finally, no significant impact of Cd was found on ADIPOQ gene expression.

3.4. Global impact of cadmium on adipocytes

Next, we investigated the effects of Cd at the transcriptomic and metabolomic levels at 1 μM by performing micro-array and untargeted

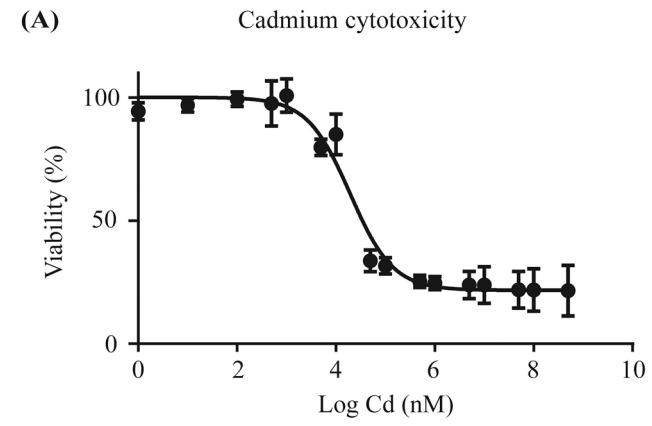

(B)

Inhibitory Concentration	Concentration (μM)
IC10	2
IC20	5
IC50	19

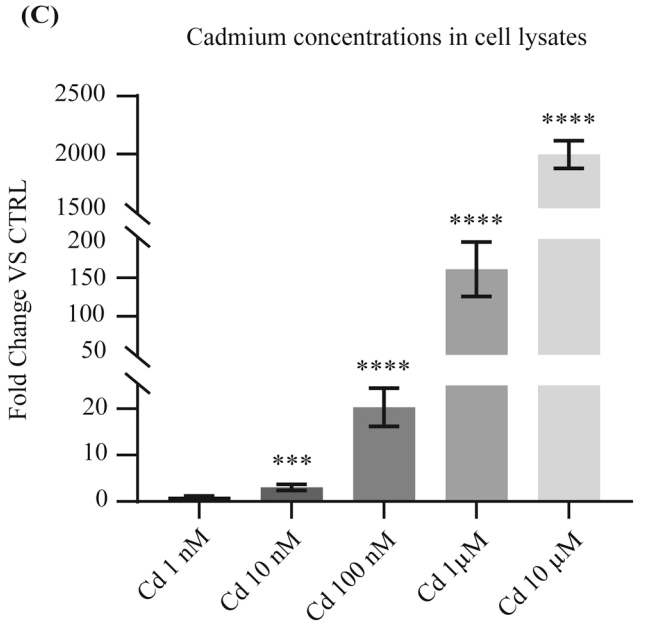

Fig. 2. Effects of cadmium exposure on AD-hMSCs viability and quantification in cells. (A) AD-hMSCs were treated with cadmium concentrations (1 nM – 500 mM) during 48 h and cell viability was measured using MTT assay. The error bars represent the standard deviation (SD). (B) The IC10, the IC20 and the IC50 of cadmium on AD-hMSCs were calculated using nonlinear regression in Graphpad Prism and are the result of two repeated experiments. After 48 h of treatment with cadmium between 1 nM and 10 μM, cadmium concentrations were measured in cellular lysates by ICP-MS (N = 5) (C). The results were expressed as the fold change between concentrations found in controls and in cadmium-treated cells. Student t-test was used to analyze the differences between controls (CTRL) and each concentration and * indicates significant changes versus controls (*** $p < 0.001$, **** $p < 0.0001$).

metabolomic experiments. Fig. 4A highlights 105 significantly upregulated and 83 significantly downregulated metabolic features (adj. p value < 0.05) by the exposure. Despite some variability in the metabolite expression pattern within the experimental groups, the heatmap highlights the clear effect linked to Cd treatment and provides a clear group clusterization. Indeed, these results does not reflect the impact of Cd on the complete metabolome but only on the detected and identified features, less specific and with milder variations compared to transcriptomic results, reflecting Cd impact on the complete transcriptome. Among the 188 impacted features, 46 were identified as metabolites using the Human Metabolome Database (HMDB) (Supplementary Table 1). Briefly, Cd strongly downregulated the levels of three main classes of metabolites: amino acids, nucleotides and fatty acids. Amino acids such as L-asparagine, L-proline, L-alanine, L-glutamine, L-leucine, L-tyrosine and L-methionine sulfoxide were downregulated and grouped in the cluster I (Fig. 4 A). In cluster II, nucleotides such as hypoxanthine, deoxycytidine and cytidine and the fatty acid 3-oxohexanoic acid were downregulated. Then, in cluster III, the decrease of uridine, adenine and adenosine was associated with the decrease of the fatty acids monoacylglycerol (16:1/0:0/0:0) and acetylcarnitine. Other fatty acids such as 3-hydroxy-tetradecanoic acid, alpha-linolenoyl ethanolamide, monoacylglycerol (0:0/18:3) and diacylglycerols (18:2/14:1), (14:0/18:3) and (18:3/14:0) were upregulated. Regarding glycerophospholipids, phosphatidylethanolamine (11D5/11M3) was increased by the treatment whereas phosphatidylcholine (18:1/20:4) was decreased. Finally, different compounds such as aldehydes, carboxylic acid and sugar like glyceraldehyde, were dysregulated by Cd exposure. At the level of gene expression, the comparison of Cd-treated versus control samples displays 1'230 upregulated and 1'239 downregulated genes (adj. p value $<$ 0.05, Fig. 4B) with a strong distinction between the two conditions of exposure and low variability in the expression pattern between replicates. The complete list of significantly impacted genes is available in Supplementary Table 2. The genes with strong statistically significant upregulation after 48 h of treatment with Cd were the metallothionein genes (MTs) and Solute Carrier Family (SLC) 30 and 39 transporters, major Zn transporters in the body. Interestingly, on Fig. 4B, we found two distinct clusters of MT and SLC genes. Cluster IV regrouped the MTs MT1B, MT1M and MT2A and the SLC transporter SLC30A1. In cluster V, the increase of SLC39A8 and SLC30A8 was correlated with the increase of MT1F, MT1L, MT1E, MT1G, MT1A, MT1X, MT1H and MT1IP.

We next explored the functional impact of Cd in adipocytes by performing pathway enrichment analysis of transcriptomic and metabolomic responses separately and by combining the two sets of data. The complete results of the over-representation pathway analyses are provided in Supplementary Table 3 (individual data sets) and in Supplementary Table 4 (combined data sets). Overall, the different over-representation pathway analyses highlighted the impact of Cd on the same pathways and the combined analysis results were kept for further discussion. Pathway analysis of combined transcriptomic and metabolomic data highlighted 78 biological pathways impacted by Cd exposure (joint q value $<$ 0.05, Fig. 4 C). Among them, Cd was found to strongly modulate cellular and protein metabolism with an impact on the metabolism of amino acids, lipids and nucleotides and on translation. In these pathways, Cd significantly downregulated the levels of amino acids, nucleotides and fatty acids (Fig. 4A). The transport of small molecules in cells was strongly dysregulated, as demonstrated by significantly affected SLC-mediated transmembrane transport (joint q value of 2.08e-14.) Cd significantly altered gene expression levels of many transporters such as SLC transporters or ATP-binding cassette transporters (ABC transporters), as well as the associated levels of amino acids, nucleotides, fatty acids and glycerophospholipids mentioned previously. These results suggested a strong impact of Cd on cellular homeostasis regulation. Moreover, many disease pathways such as Non-alcoholic fatty liver disease, Central carbon and Choline metabolism in cancer were significantly impacted, due to the alteration of SLC transporters, diacylglycerols, phosphatidylethanolamine (11D5/11M3) and phosphatidylcholine (18:1/20:4). Cd also affected copper and Zn homeostasis, cellular response to metal ions and Metallothioneins bind metals pathways, with a major impact on genes such as SLCs and MTs. Finally, Cd was able to alter various pathways of DNA repair and signal transduction and interestingly, the pathway of Regulation of lipolysis in

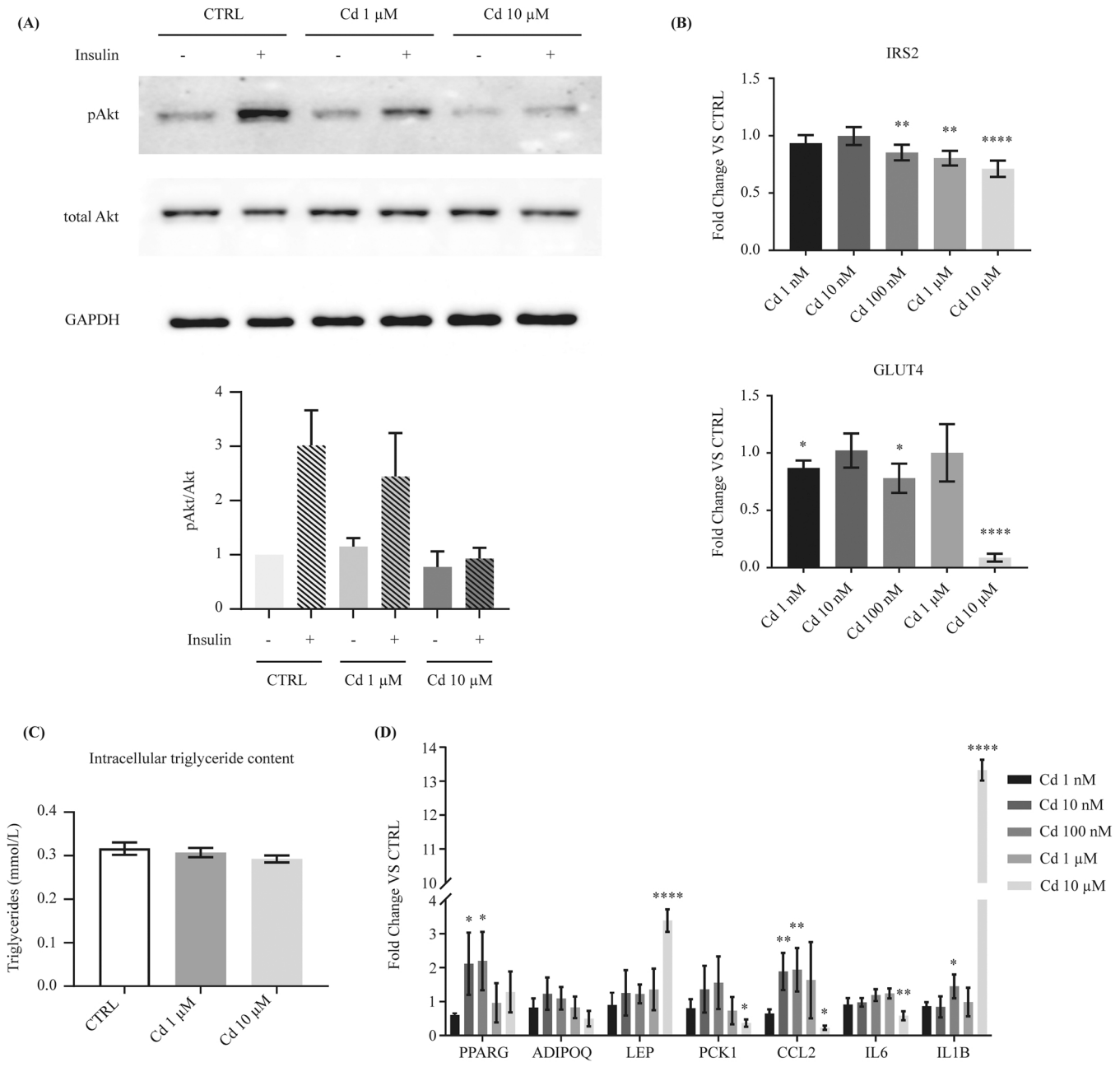

Fig. 3. Assessment of the effects of cadmium on cell functional characteristics and adipocyte genes. (A) Western-blots of phosphorylated and total Akt in protein samples from AD-hMSCs treated with two cadmium concentrations (1 µM and 10 µM) or control for 48 h, followed by insulin stimulation for 15 min at 10 nM. GADPH was used as an internal loading control. Relative quantification was calculated as the ratio of phospho-Akt and Akt and data are represented as mean and standard deviation of two independent experiments. (B) mRNA levels of two genes involved in the insulin signaling pathway, IRS2 and GLUT4, in AD-hMSCs treated with cadmium for 48 h. (C) Intracellular triglyceride content (N = 8) in AD-hMSCs treated with the two highest concentrations of cadmium, 1 µM and 10 µM, for 48 h. Student t-test was used to analyze the differences between controls (CTRL) and each concentration. The error bars represent the standard errors (SE). (D) mRNA levels of genes markers of the adipocyte function and inflammation in AD-hMSC adipocytes treated with cadmium during 48 h. mRNA expression levels were normalized as a ratio to the corresponding RPS13 mRNA expression level. Relative expression and fold change were expressed between controls (N = 11) and cadmium treated cells (N = 5). Student t-test was used to analyze the differences between control and cadmium conditions and * indicates significant changes versus controls (* $p < 0.05$, ** $p < 0.01$, **** $p < 0.0001$).

adipocytes with the dysregulation of Fatty Acid Binding Protein 4 (FABP4) gene.

3.5. Perturbations of trace element homeostasis by cadmium

We further explored the functional effect of Cd-induced perturbations on genes involved in SLC-mediated transmembrane transport. Modulations of two Zn transporters, SLC30A1 and SLC39A8, and three MTs, MT2A, MT1A and MT1B were confirmed by RT-qPCR. Importantly, besides their implication in the protection of cells against heavy metal toxicity, MTs are also involved in the transport of physiological trace elements across the cells (Yang and Shu, 2015). At the Zn transporter level, Cd treatment significantly increased the gene expression level of SLC39A8 at 10 µM and of SLC30A1 from 1 µM (Fig. 5A). Moreover, a mild decrease of SLC39A9 mRNA level was observed at 10 nM. The mRNA level of MT2A was significantly increased from 100 nM (Fig. 5B).

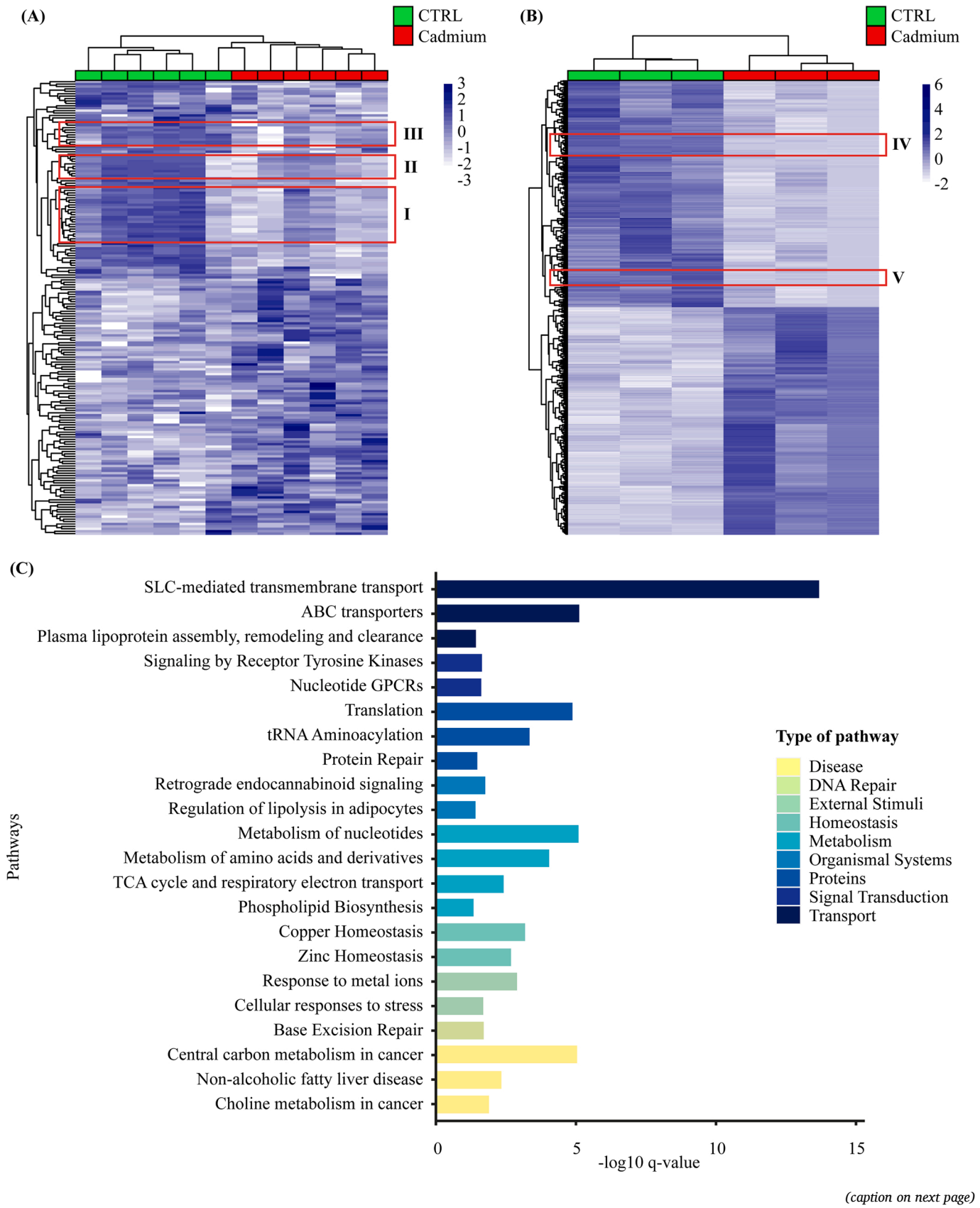

(caption on next page)

Fig. 4. Cadmium exposure (48 h at 1 μM) induces transcriptomic and metabolomic changes in mature AD-hMSCs. Representation of all the significant metabolites (A) and genes (B) altered by cadmium treatment. The data were clustered by Ward's clustering with the Euclidean distance in R. Heatmap columns represent control and cadmium-treated cells and rows represent significantly dysregulated metabolites and genes. The heatmaps show the two clusters of metabolites and genes up- or downregulated by the treatment. For metabolites, the statistical significances between controls and cadmium-treated cells (N = 6) were assessed using Spearman correlation in R (adj. p value < 0.05). For each gene, the fold change between control and cadmium samples (N = 3) was calculated and statistical significance of differences in means from the controls was calculated using LIMMA package in R. Differences were considered significant if the fold change was > 1.5 and the adj. p value was < 0.05. (A) The clusters I, II and III highlight three of the main classes of impacted metabolites such as amino acids, nucleotides and fatty acids. (B) The clusters IV and V show some of the most impacted genes, metallothioneins and the SLC transporters. (C) Over-representation pathway analysis of some of the most significantly altered biological pathways enriched by genes and metabolites at 1 μM (joint q value < 0.05). The bars represent the joint q-value corresponding to each pathway.

MT1A and MT1B mRNA levels were significantly increased from 1 μM. To complete our understanding on how Cd can affect cellular trace element homeostasis in adipocytes, we quantified 14 trace elements by ICP-MS. No alteration of the concentrations of lithium, aluminum, chromium, cobalt, nickel, arsenic, selenium, molybdenum, antimony, lead and bismuth was observed in cells and cellular media (Supplementary Fig. 1). At 10 μM of Cd, copper levels significantly increased in cells and media and significantly decreased in cell media at 1 μM (Supplementary Fig. 1). A significant decrease in cell lysates and a significant increase in cell media were observed for Zn at 10 μM of Cd (Fig. 5C). On the contrary, we observed a significant increase in cellular manganese from 1 μM (Fig. 5D) and a significant decrease in cell media manganese concentrations at 10 μM.

Overall, all these results highlighted various metabolic perturbations induced by Cd at non-toxic concentrations, 1 μM. Such effects are exacerbated and confirmed at increased Cd concentrations, although we cannot exclude that a general toxicity also contribute to some of the observations performed at 10 μM.

4. Discussion

Adipose tissue is a potential site of accumulation of toxicants, including trace elements. In this study, we quantified Cd concentrations found in post-mortem human SAT and VAT and highlighted their positive correlation with sex, age and smoking status and a negative correlation with BMI. In contrast, Cd levels were not associated with PMI. This observation is of high relevance, as Cd is strongly subjected to post-mortem redistribution in other biological matrices, such as blood and urine (Goullé et al., 2007). Here, the absence of correlation of adipose tissue Cd levels with PMI suggests that our post-mortem measurements are likely reflecting Cd ante-mortem deposition, similarly to what is known for the ante-mortem deposition of drugs in adipose tissue (Levisky et al., 2001). This is further sustained by the observations of Echeverria et al. (2019) who found the same associations of Cd with sex, age, BMI and smoking status in adipose tissue samples collected from living samples. Indeed, Cd concentrations were significantly higher not only in women adipose tissue but also in blood, urine and kidneys (Vahter et al., 2007), as compared to men. This might be due to increased absorption and exposure or skeletal changes associated with pregnancy, lactation or menopause (Vahter et al., 2002). Various studies already highlighted the associations between Cd levels in urine, blood and age (Amzal et al., 2009; Lopez-Herranz et al., 2016; Sun et al., 2016), shedding light on the accumulative potential of this heavy metal in different biological samples. Moreover, cigarettes are the predominant source of Cd exposure (Milnerowicz et al., 2015) and smokers have significant levels of Cd in blood (Heitland and Koster, 2006), urine (Bochud et al., 2018) and adipose tissue (Echeverria et al., 2019). Interestingly, in our study, we found a positive correlation between Cd levels and smoking status in SAT. Finally, Cd levels were negatively correlated with BMI in adipose tissues, in agreement with Echeverria et al. (2019) data, who suggested a potential dilution of Cd concentrations in case of high level of obesity.

Our study also revealed that an acute in vitro exposure to Cd, at concentrations that are relevant for an environmental exposure, was able to activate cell defense mechanism in human mature adipocytes and to dysregulate cellular response upon insulin stimulation and adipocyte genes. These effects were observed at concentrations below the IC50 and IC10, which were calculated at 19 μM and 2 μM, respectively. According to previous reports on non-differentiated AD-hMSCs, Cd treatment determined IC50s between 14 and 56 μM (Alkharashi et al., 2018, 2019). So far, most of the studies about the impact of Cd on adipocytes in vitro focused on the differentiation process rather than its effects on mature adipocytes. In differentiating 3T3-L1 mouse adipocytes, Cd treatment inhibited preadipocyte differentiation (Lee et al., 2012; Rosen et al., 1999). Of note, these observations were obtained at Cd concentrations comparable to those found in our study in human adipose tissues. Our study shows that Cd as an impact also on mature adipocytes. Indeed, in AD-hMSCs already differentiated into adipocytes, we observed a mild increase of PPARG expression and a dysregulation of fatty acid levels, highlighting the potential impact of Cd on fatty acid homeostasis. Interestingly, over-representation pathway analysis revealed the impact of Cd on the regulation of lipolysis in adipocytes, associated with the significant increase of FABP4 gene. FABP4 is involved in fatty acid metabolism, uptake and transport in adipocytes (Furuhashi et al., 2014) and can play a role in the development of insulin resistance. Increased circulating levels of FABP4 is already positively associated with obesity, insulin resistance, T2D and atherosclerosis (Furuhashi et al., 2014). To support this result, we found a strong dysregulation of insulin signaling pathway with a decreased Akt phosphorylation after insulin stimulation with Cd 10 μM treatment and a significant decrease of IRS2 and GLUT4 genes. Importantly, downregulated expression of GLUT4 (Chadt and Al-Hasani, 2020; Garvey et al., 1991) and IRS2 (Brady, 2004) genes are also associated with the development of obesity and insulin resistance. Moreover, we found a significant decrease of PCK1 gene, involved in the production of glycerol necessary for triglyceride synthesis in adipose tissue (Millward et al., 2010; Nye et al., 2008), although without significant decrease in triglyceride content. This suggests that Cd perturbs lipid metabolism in mature adipocytes, even if further investigations might help identifying which lipid classes are particularly impacted. Altogether, these observations highlight the impact of Cd on fat storage and glucose metabolism and the potential implication of Cd exposure in the development of obesity, insulin resistance and T2D. In addition, Cd activated the pro-inflammatory response of cells with the significant increase of LEP and the two cytokines CCL2 and IL1B, as also supported by the impact of Cd on phosphatidylethanolamine (11D5/11M3). Indeed, phosphatidylethanolamine lipids are significantly higher in obese and insulin-resistant adipose tissue, which developed inflammation (Wentworth et al., 2016). These results raise the question about the possible effects of a more chronic exposure with Cd accumulation in adipose tissues on the pro-inflammatory state of the adipocytes.

Another key observation of our study is that Cd acute exposure, at concentrations consistent with the environmentally relevant ones, induced a strong dysregulation of cellular homeostasis. In particular, we highlighted the impact of Cd on the homeostasis of Zn, an essential trace element involved in many cellular processes (Hojyo and Fukada, 2016), immune function and inflammation (Rink and Gabriel, 2000). Of note, alteration of Zn levels might participate to the development of obesity, insulin resistance (Tinkov et al., 2015) and T2D (Viktorinova et al., 2009), by modifying the release of free fatty acids and glucose uptake

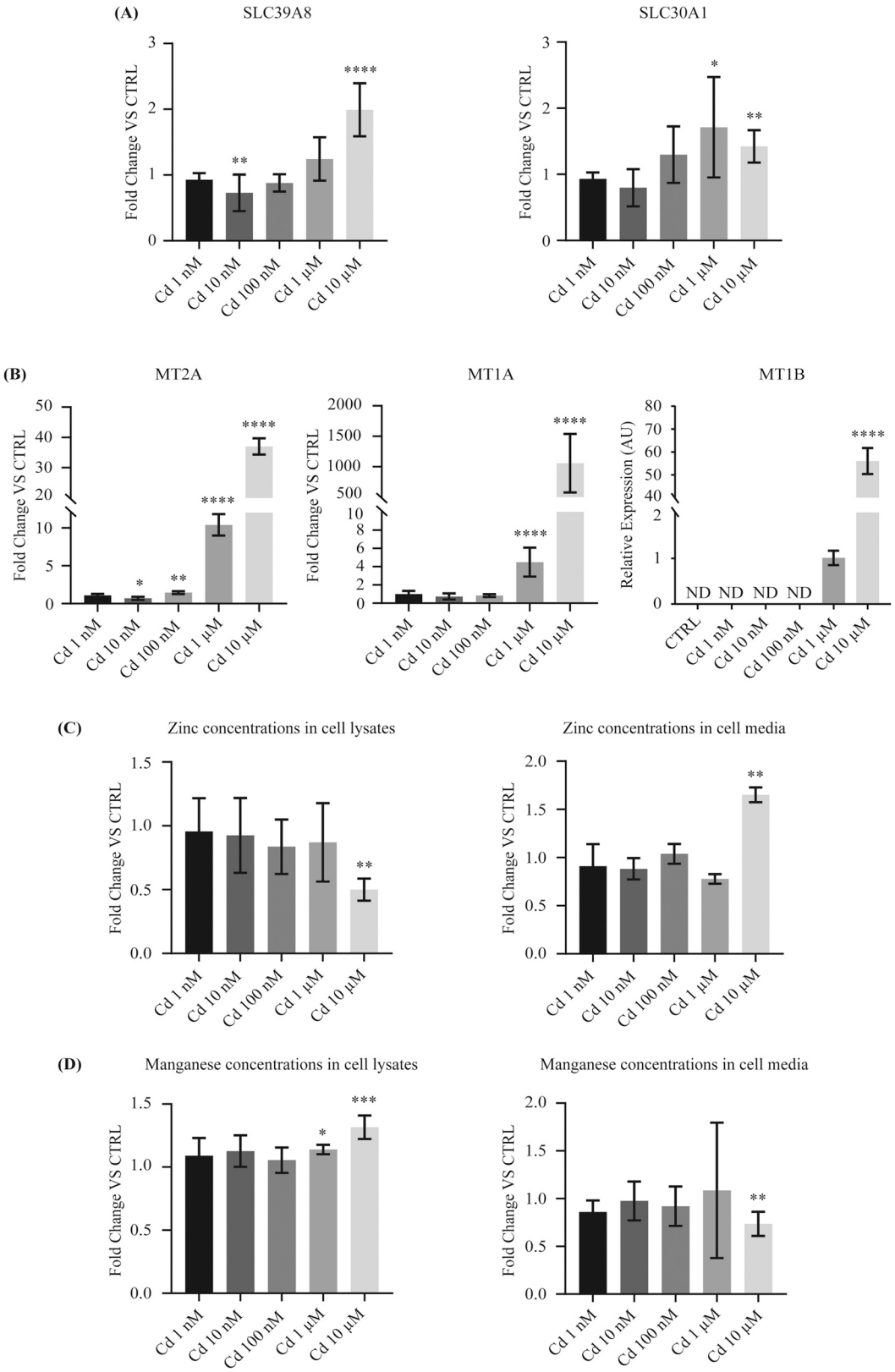

Fig. 5. Effects of cadmium on zinc transporters and homeostasis. 48 h of cadmium exposure (1 nM to 10 µM, N = 5) on AD-hMSCs induces changes in mRNA levels of two Zn transporters (A), SLC39A8 and SLC30A1, and leads to the induction of metallothioneins (B), MT2A, MT1A and MT1B. mRNA level was normalized as a ratio to the corresponding RPS13 mRNA level. Relative expression and fold change were expressed between controls and cadmium-treated cells. For MT1B, mRNA levels were not detected (ND) in controls and up to cadmium 100 nM treatment. Results were expressed as the relative expression between 1 µM and 10 µM. Zinc (C) and manganese (D) were quantified by ICP-MS in cellular lysates and media (N = 5). The results were expressed as the fold change between controls and cadmium-treated cells. Student t-test was used to analyze the differences between controls and each concentration and * indicates changes versus controls. For MT1B, statistical significance analysis was made by Student t-test between the two cadmium conditions. (* $p < 0.05$, ** $p < 0.01$, *** $p < 0.001$, **** $p < 0.0001$).

(Fukunaka and Fujitani, 2018). Zn transporters, such as MTs and SLCs (Yang and Shu, 2015), are upregulated during adipogenesis (Smidt et al., 2007). In our study, we found that SLC39A8, SLC39A14 and SLC30A8 were significantly increased by Cd treatment, in concomitance with decreased Zn concentration in cells, suggesting a direct impact of Cd on Zn transport. Cd can compete with physiological metal ions to enter the cells and inhibit their transport (Fujishiro and Himeno, 2019; Thevenod et al., 2019) and the SLC39A14 transporter was found to have a high affinity for Cd^{2+} ions (Thevenod et al., 2019). In addition, the SLC39A8 transporter is abundantly expressed in the tissues where Cd accumulates, such as kidneys, liver and adipose tissue (Thevenod et al., 2019). In parallel, Cd strongly induced metallothioneins, a class of cysteine-rich proteins involved in the homeostasis and transport of physiological metal ions (Kayaalti et al., 2011), but also in the protection of cells against heavy metal cytotoxicity. Our observation is consistent with previous studies showing that Cd is able to induce the expression of MTs in kidneys and liver (Revis and Osborne, 1984), but also in adipose tissue (Kawakami et al., 2010). MT2A was upregulated at a lower concentration than MT1A and MT1B, suggesting that, in this tissue, this protein is the first to respond to Cd exposure. In line with this observation, MT2A is the most expressed MT in human body and is increased in response to various stimuli (Kayaalti and Soylemezoglu, 2010). The strong impact of Cd on Zn homeostasis in human mature adipocytes raises questions about the effect of Cd on systemic trace element homeostasis and a potential link with the risk of obesity and T2D development. Finally, our observations reveal new mechanisms potentially underlying the metabolic effects induced by Cd chronic exposure in humans.

5. Conclusion

In our study, we revealed that Cd acute exposure induces various metabolomic and transcriptomic perturbations in adipocytes at concentration levels found in human adipose tissue. Cd induced pro-inflammatory genes, perturbed adipocyte functions and strongly dysregulated small molecule homeostasis and transport. In particular, we demonstrated that Cd had a severe impact on key SLC-transporters and MTs mediating trace element ion transport and involved in many metabolic diseases. These results give mechanistic foundations to understand the ability of Cd to induce cellular homeostasis perturbations and to explain why population exposed to Cd might be more prone to develop various metabolic complications.

Declaration of Competing Interest

The authors declare that they have no known competing financial interests or personal relationships that could have appeared to influence the work reported in this paper.

Data availability statement

Metabolomic data are available in Metabolights database with the following ID: MTBLS4128.

Microarray data are deposited in GEO at the accession number GSE193390.

Acknowledgments

This research was supported by Swiss National Science Foundation [grant #31003A-182420]. We thank the Institute of Genetics and Genomics of the University of Geneva for their analyses of the transcriptomic data.

Appendix A. Supporting information

Supplementary data associated with this article can be found in the online version at doi:10.1016/j.tox.2022.153153.

References

Afridi, H.I., Kazi, T.G., Kazi, N., Jamali, M.K., Arain, M.B., Jalbani, N., Baig, J.A., Sarfraz, R.A., 2008. Evaluation of status of toxic metals in biological samples of diabetes mellitus patients. Diabetes Res. Clin. Pract. 80, 280–288. https://doi.org/10.1016/j.diabres.2007.12.021.

Akalestou, E., Genser, L., Rutter, G.A., 2020. Glucocorticoid metabolism in obesity and following weight loss. Front. Endocrinol. 11, 59. https://doi.org/10.3389/fendo.2020.00059.

Alkharashi, N.A.O., Periasamy, V.S., Athinarayanan, J., Alshatwi, A.A., 2018. Assessment of sulforaphane-induced protective mechanisms against cadmium toxicity in human mesenchymal stem cells. Environ. Sci. Pollut. Res. Int. 25, 10080–10089. https://doi.org/10.1007/s11356-018-1228-7.

Alkharashi, N.A.O., Periasamy, V.S., Athinarayanan, J., Alshatwi, A.A., 2019. Sulforaphane alleviates cadmium-induced toxicity in human mesenchymal stem cells through POR and TNFSF10 genes expression. Biomed. Pharmacother. 115, 108896 https://doi.org/10.1016/j.biopha.2019.108896.

Amzal, B., Julin, B., Vahter, M., Wolk, A., Johanson, G., Akesson, A., 2009. Population toxicokinetic modeling of cadmium for health risk assessment. Environ Health Perspect. 117, 1293–1301. https://doi.org/10.1289/ehp.0800317.

Bararpour, N., Gilardi, F., Carmeli, C., Sidibe, J., Ivanisevic, J., Caputo, T., Augsburger, M., Grabherr, S., Desvergne, B., Guex, N., Bochud, M., Thomas, A., 2021. DBnorm as an R package for the comparison and selection of appropriate statistical methods for batch effect correction in metabolomic studies. Sci. Rep. 11, 5657. https://doi.org/10.1038/s41598-021-84824-3.

Barregard, L., Sallsten, G., Fagerberg, B., Borne, Y., Persson, M., Hedblad, B., Engstrom, G., 2016. Blood cadmium levels and incident cardiovascular events during follow-up in a population-based cohort of Swedish adults: the malmo diet and cancer study. Environ. Health Perspect. 124, 594–600. https://doi.org/10.1289/ehp.1509735.

Bochud, M., Jenny-Burri, J., Pruijm, M., Ponte, B., Guessous, I., Ehret, G., Petrovic, D., Dudler, V., Haldimann, M., Escher, G., Dick, B., Mohaupt, M., Paccaud, F., Burnier, M., Pechere-Bertschi, A., Martin, P.Y., Vogt, B., Ackermann, D., 2018. Urinary cadmium excretion is associated with increased synthesis of cortico- and sex steroids in a population study. J. Clin. Endocrinol. Metab. 103, 748–758. https://doi.org/10.1210/jc.2017-01540.

Brady, M.J., 2004. IRS2 takes center Stage in the development of type 2 diabetes. J. Clin. Investig. 114, 886–888. https://doi.org/10.1172/jci200423108.

Chadt, A., Al-Hasani, H., 2020. Glucose transporters in adipose tissue, liver, and skeletal muscle in metabolic health and disease. Pflug Arch. 472, 1273–1298. https://doi.org/10.1007/s00424-020-02417-x.

Chambers, M.C., Maclean, B., Burke, R., Amodei, D., Ruderman, D.L., Neumann, S., Gatto, L., Fischer, B., Pratt, B., Egertson, J., Hoff, K., Kessner, D., Tasman, N., Shulman, N., Frewen, B., Baker, T.A., Brusniak, M.Y., Paulse, C., Creasy, D., Flashner, L., Kani, K., Moulding, C., Seymour, S.L., Nuwaysir, L.M., Lefebvre, B., Kuhlmann, F., Roark, J., Rainer, P., Detlev, S., Hemenway, T., Huhmer, A., Langridge, J., Connolly, B., Chadick, T., Holly, K., Eckels, J., Deutsch, E.W., Moritz, R.L., Katz, J.E., Agus, D.B., MacCoss, M., Tabb, D.L., Mallick, P., 2012. A cross-platform toolkit for mass spectrometry and proteomics. Nat. Biotechnol. 30, 918–920. https://doi.org/10.1038/nbt.2377.

Chen, Y.W., Yang, C.Y., Huang, C.F., Hung, D.Z., Leung, Y.M., Liu, S.H., 2009. Heavy metals, islet function and diabetes development. Islets 1, 169–176. https://doi.org/10.4161/isl.1.3.9262.

Coelho, P., Costa, S., Costa, C., Silva, S., Walter, A., Ranville, J., Pastorinho, M.R., Harrington, C., Taylor, A., Dall'Armi, V., Zoffoli, R., Candeias, C., da Silva, E.F., Bonassi, S., Laffon, B., Teixeira, J.P., 2014. Biomonitoring of several toxic metal (loid)s in different biological matrices from environmentally and occupationally exposed populations from Panasqueira mine area, Portugal. Environ. Geochem. Health 36, 255–269. https://doi.org/10.1007/s10653-013-9562-7.

Dufau, J., Shen, J.X., Couchet, M., De Castro Barbosa, T., Mejhert, N., Massier, L., Griseti, E., Mouisel, E., Amri, E.Z., Lauschke, V.M., Ryden, M., Langin, D., 2021. In vitro and ex vivo models of adipocytes. Am. J. Physiol. Cell Physiol. 320, C822–C841. https://doi.org/10.1152/ajpcell.00519.2020.

Echeverria, R., Vrhovnik, P., Salcedo-Bellido, I., Iribarne-Duran, L.M., Fiket, Z., Dolenec, M., Martin-Olmedo, P., Olea, N., Arrebola, J.P., 2019. Levels and determinants of adipose tissue cadmium concentrations in an adult cohort from Southern Spain. Sci. Total Environ. 670, 1028–1036. https://doi.org/10.1016/j.scitotenv.2019.03.114.

Egger, A.E., Grabmann, G., Gollmann-Tepekoylu, C., Pechriggl, E.J., Artner, C., Turkcan, A., Hartinger, C.G., Fritsch, H., Keppler, B.K., Brenner, E., Grimm, M., Messner, B., Bernhard, D., 2019. Chemical imaging and assessment of cadmium distribution in the human body. Metallomics 11, 2010–2019. https://doi.org/10.1039/c9mt00178f.

Fantuzzi, G., 2005. Adipose tissue, adipokines, and inflammation. J. Allergy Clin. Immunol. 115, 911–919. https://doi.org/10.1016/j.jaci.2005.02.023 quiz 920.

Freire, C., Vrhovnik, P., Fiket, Z., Salcedo-Bellido, I., Echeverria, R., Martin-Olmedo, P., Kniewald, G., Fernandez, M.F., Arrebola, J.P., 2020. Adipose tissue concentrations of arsenic, nickel, lead, tin, and titanium in adults from GraMo cohort in Southern Spain: an exploratory study. Sci. Total Environ. 719, 137458 https://doi.org/10.1016/j.scitotenv.2020.137458.

Fujishiro, H., Himeno, S., 2019. New insights into the roles of ZIP8, a cadmium and manganese transporter, and its relation to human diseases. Biol. Pharm. Bull. 42, 1076–1082. https://doi.org/10.1248/bpb.b18-00637.

Fukunaka, A., Fujitani, Y., 2018. Role of zinc homeostasis in the pathogenesis of diabetes and obesity. Int. J. Mol. Sci. 19 https://doi.org/10.3390/ijms19020476.
Furuhashi, M., Saitoh, S., Shimamoto, K., Miura, T., 2014. Fatty acid-binding protein 4 (FABP4): pathophysiological insights and potent clinical biomarker of metabolic and cardiovascular diseases. Clin. Med. Insights Cardiol. 8, 23–33. https://doi.org/10.4137/CMC.S17067.
Garvey, W.T., Maianu, L., Huechsteadt, T.P., Birnbaum, M.J., M, M.J., Ciaraldi, T.P., 1991. Pretranslational suppression of a glucose transporter protein causes insulin resistance in adipocytes from patients with non-insulin-dependent diabetes mellitus and obesity. J. Clin. Investig. 87, 1072–1081. https://doi.org/10.1172/JCI115068.
Genchi, G., Sinicropi, M.S., Lauria, G., Carocci, A., Catalano, A., 2020. The effects of cadmium toxicity. Int. J. Environ. Res. Public Health 17. https://doi.org/10.3390/ijerph17113782.
Goullé, J.-P., Mahieu, L., Maignant, V., Bouige, D., Saussereau, É., Lacroix, C., 2007. Valeurs usuelles des métaux et métalloïdes dans le sang total et les urines par ICP-MS chez cinquante-quatre sujets décédés. Ann. Toxicol. Anal. 19, 43–51. https://doi.org/10.1051/ata:2007007.
Heitland, P., Koster, H.D., 2006. Biomonitoring of 37 trace elements in blood samples from inhabitants of northern Germany by ICP-MS. J. Trace Elem. Med. Biol. 20, 253–262. https://doi.org/10.1016/j.jtemb.2006.08.001.
Hellstrom, L., Elinder, C.G., Dahlberg, B., Lundberg, M., Jarup, L., Persson, B., Axelson, O., 2001. Cadmium exposure and end-stage renal disease. Am. J. Kidney Dis. 38, 1001–1008. https://doi.org/10.1053/ajkd.2001.28589.
Hojyo, S., Fukada, T., 2016. Roles of zinc signaling in the immune system. J. Immunol. Res. 2016, 6762343 https://doi.org/10.1155/2016/6762343.
Jafari, P., Thomas, A., Haselbach, D., Watfa, W., Pantet, O., Michetti, M., Raffoul, W., Applegate, L.A., Augsburger, M., Berger, M.M., 2018. Trace element intakes should be revisited in burn nutrition protocols: a cohort study. Clin. Nutr. 37, 958–964. https://doi.org/10.1016/j.clnu.2017.03.028.
Janesick, A., Blumberg, B., 2011. Endocrine disrupting chemicals and the developmental programming of adipogenesis and obesity. Birth Defects Res. C Embryo Today 93, 34–50. https://doi.org/10.1002/bdrc.20197.
Janesick, A.S., Blumberg, B., 2016. Obesogens: an emerging threat to public health. Am. J. Obstet. Gynecol. 214, 559–565. https://doi.org/10.1016/j.ajog.2016.01.182.
Kamburov, A., Cavill, R., Ebbels, T.M., Herwig, R., Keun, H.C., 2011. Integrated pathway-level analysis of transcriptomics and metabolomics data with IMPaLA. Bioinformatics 27, 2917–2918. https://doi.org/10.1093/bioinformatics/btr499.
Kawakami, T., Sugimoto, H., Furuichi, R., Kadota, Y., Inoue, M., Setsu, K., Suzuki, S., Sato, M., 2010. Cadmium reduces adipocyte size and expression levels of adiponectin and Peg1/Mest in adipose tissue. Toxicology 267, 20–26. https://doi.org/10.1016/j.tox.2009.07.022.
Kayaalti, Z., Aliyev, V., Soylemezoglu, T., 2011. The potential effect of metallothionein ^{2}A–^{5}A/G single nucleotide polymorphism on blood cadmium, lead, zinc and copper levels. Toxicol. Appl. Pharmacol. 256, 1–7. https://doi.org/10.1016/j.taap.2011.06.023.
Kayaalti, Z., Mergen, G., Soylemezoglu, T., 2010. Effect of metallothionein core promoter region polymorphism on cadmium, zinc and copper levels in autopsy kidney tissues from a Turkish population. Toxicol. Appl. Pharmacol. 245, 252–255. https://doi.org/10.1016/j.taap.2010.03.007.
Kayaalti, Z., Soylemezoglu, T., 2010. The polymorphism of core promoter region on metallothionein 2A-metal binding protein in Turkish population. Mol. Biol. Rep. 37, 185–190. https://doi.org/10.1007/s11033-009-9586-3.
Kershaw, E.E., Schupp, M., Guan, H.P., Gardner, N.P., Lazar, M.A., Flier, J.S., 2007. PPARgamma regulates adipose triglyceride lipase in adipocytes in vitro and in vivo. Am. J. Physiol. Endocrinol. Metab. 293, E1736–E1745. https://doi.org/10.1152/ajpendo.00122.2007.
Lee, E.J., Moon, J.Y., Yoo, B.S., 2012. Cadmium inhibits the differentiation of 3T3-L1 preadipocyte through the C/EBPalpha and PPARgamma pathways. Drug Chem. Toxicol. 35, 225–231. https://doi.org/10.3109/01480545.2011.591401.
Levisky, J.A., Bowermann, D.L., Jenkins, W.W., Johnson, D.G., Karch, S.B., 2001. Drugs in postmortem adipose tissues: evidence of antemortem deposition. Forensic Sci. Int. 121, 157–160.
Longo, M., Zatterale, F., Naderi, J., Parrillo, L., Formisano, P., Raciti, G.A., Beguinot, F., Miele, C., 2019. Adipose tissue dysfunction as determinant of obesity-associated metabolic complications. Int. J. Mol. Sci. 20 https://doi.org/10.3390/ijms20092358.
Lopez-Herranz, A., Cutanda, F., Esteban, M., Pollan, M., Calvo, E., Perez-Gomez, B., Victoria Cortes, M., Castano, A., Bioambient, Es, 2016. Cadmium levels in a representative sample of the Spanish adult population: the BIOAMBIENT.ES project. J. Expo. Sci. Environ. Epidemiol. 26, 471–480. https://doi.org/10.1038/jes.2015.25.
Millward, C.A., Desantis, D., Hsieh, C.W., Heaney, J.D., Pisano, S., Olswang, Y., Reshef, L., Beidelschies, M., Puchowicz, M., Croniger, C.M., 2010. Phosphoenolpyruvate carboxykinase (Pck1) helps regulate the triglyceride/fatty acid cycle and development of insulin resistance in mice. J. Lipid Res. 51, 1452–1463. https://doi.org/10.1194/jlr.M005363.
Milnerowicz, H., Sciskalska, M., Dul, M., 2015. Pro-inflammatory effects of metals in persons and animals exposed to tobacco smoke. J. Trace Elem. Med. Biol. 29, 1–10. https://doi.org/10.1016/j.jtemb.2014.04.008.
Nye, C.K., Hanson, R.W., Kalhan, S.C., 2008. Glyceroneogenesis is the dominant pathway for triglyceride glycerol synthesis in vivo in the rat. J. Biol. Chem. 283, 27565–27574. https://doi.org/10.1074/jbc.M804393200.
OECD, 2019. The Heavy Burden of Obesity: The Economics of Prevention. OECD Health Policy Studies. OECD Publishing,, Paris. https://doi.org/10.1787/67450d67-en.
Park, J.D., Zheng, W., 2012. Human exposure and health effects of inorganic and elemental mercury. J. Prev. Med. Public Health 45, 344–352. https://doi.org/10.3961/jpmph.2012.45.6.344.
Revis, N.W., Osborne, T.R., 1984. Dietary Protein Effects on Cadmium and Metallothionein accumulation in the liver and kidney of rats. Environ. Health Perspect. 54, 83–91. https://doi.org/10.1289/ehp.845483.
Rink, L., Gabriel, P., 2000. Zinc and the immune system. Proc. Nutr. Soc. 59, 541–552. https://doi.org/10.1017/s0029665100000781.
Ritchie, M.E., Phipson, B., Wu, D., Hu, Y., Law, C.W., Shi, W., Smyth, G.K., 2015. limma powers differential expression analyses for RNA-sequencing and microarray studies. Nucleic Acids Res. 43, e47 https://doi.org/10.1093/nar/gkv007.
Rosen, E.D., Sarraf, P., Troy, A.E., Bradwin, G., Moore, K., Milstone, D.S., Spiegelman, B. M., Mortensen, R.M., 1999. PPARg is required for the differentiation of adipose tissue in vivo and in vitro. Mol. Cell 4, 611–617. https://doi.org/10.1016/s1097-2765(00)80211-7.
Satarug, S., Garrett, S.H., Sens, M.A., Sens, D.A., 2010. Cadmium, environmental exposure, and health outcomes. Environ. Health Perspect. 118, 182–190. https://doi.org/10.1289/ehp.0901234.
Schneider, C.A., Rasband, W.S., Eliceiri, K.W., 2012. NIH Image to ImageJ: 25 years of image analysis. Nature Methods 9, 671–675.
Smidt, K., Pedersen, S.B., Brock, B., Schmitz, O., Fisker, S., Bendix, J., Wogensen, L., Rungby, J., 2007. Zinc-transporter genes in human visceral and subcutaneous adipocytes: lean versus obese. Mol. Cell Endocrinol. 264, 68–73. https://doi.org/10.1016/j.mce.2006.10.010.
Sun, H., Wang, D., Zhou, Z., Ding, Z., Chen, X., Xu, Y., Huang, L., Tang, D., 2016. Association of cadmium in urine and blood with age in a general population with low environmental exposure. Chemosphere 156, 392–397. https://doi.org/10.1016/j.chemosphere.2016.05.013.
Świderska, E., Strycharz, J., Wróblewski, A., Szemraj, J., Drzewoski, J. and Śliwińska, A. 2020. Role of PI3K/AKT Pathway in Insulin-Mediated Glucose Uptake. Blood Glucose Levels.
Tellez-Plaza, M., Navas-Acien, A., Menke, A., Crainiceanu, C.M., Pastor-Barriuso, R., Guallar, E., 2012. Cadmium exposure and all-cause and cardiovascular mortality in the U.S. general population. Environ. Health Perspect. 120, 1017–1022. https://doi.org/10.1289/ehp.1104352.
Thevenod, F., Fels, J., Lee, W.K., Zarbock, R., 2019. Channels, transporters and receptors for cadmium and cadmium complexes in eukaryotic cells: myths and facts. Biometals 32, 469–489. https://doi.org/10.1007/s10534-019-00176-6.
Tinkov, A.A., Sinitskii, A.I., Popova, E.V., Nemereshina, O.N., Gatiatulina, E.R., Skalnaya, M.G., Skalny, A.V., Nikonorov, A.A., 2015. Alteration of local adipose tissue trace element homeostasis as a possible mechanism of obesity-related insulin resistance. Med. Hypotheses 85, 343–347. https://doi.org/10.1016/j.mehy.2015.06.005.
Vahter, M., Akesson, A., Liden, C., Ceccatelli, S., Berglund, M., 2007. Gender differences in the disposition and toxicity of metals. Environ. Res. 104, 85–95. https://doi.org/10.1016/j.envres.2006.08.003.
Vahter, M., Berglund, M., Akesson, A., Liden, C., 2002. Metals and women's health. Environ. Res. 88, 145–155. https://doi.org/10.1006/enrs.2002.4338.
Viktorinova, A., Toserova, E., Krizko, M., Durackova, Z., 2009. Altered metabolism of copper, zinc, and magnesium is associated with increased levels of glycated hemoglobin in patients with diabetes mellitus. Metabolism 58, 1477–1482. https://doi.org/10.1016/j.metabol.2009.04.035.
Wallia, A., Allen, N.B., Badon, S., El Muayed, M., 2014. Association between urinary cadmium levels and prediabetes in the NHANES 2005-2010 population. Int. J. Hyg. Environ. Health 217, 854–860. https://doi.org/10.1016/j.ijheh.2014.06.005.
Wentworth, J.M., Naselli, G., Ngui, K., Smyth, G.K., Liu, R., O'Brien, P.E., Bruce, C., Weir, J., Cinel, M., Meikle, P.J., Harrison, L.C., 2016. GM3 ganglioside and phosphatidylethanolamine-containing lipids are adipose tissue markers of insulin resistance in obese women. Int. J. Obes. 40, 706–713. https://doi.org/10.1038/ijo.2015.223.
Yang, H., Shu, Y., 2015. Cadmium transporters in the kidney and cadmium-induced nephrotoxicity. Int. J. Mol. Sci. 16, 1484–1494. https://doi.org/10.3390/ijms16011484.
Yang, Q., Wang, Y., Zhang, Y., Li, F., Xia, W., Zhou, Y., Qiu, Y., Li, H., Zhu, F., 2020. NOREVA: enhanced normalization and evaluation of time-course and multi-class metabolomic data. Nucleic Acids Res. 48, W436–W448. https://doi.org/10.1093/nar/gkaa258.
Yedomon, B., Menudier, A., Etangs, F.L.D., Anani, L., Fayomi, B., Druet-Cabanac, M., Moesch, C., 2017. Biomonitoring of 29 trace elements in whole blood from inhabitants of Cotonou (Benin) by ICP-MS. J. Trace Elem. Med. Biol. 43, 38–45. https://doi.org/10.1016/j.jtemb.2016.11.004.
Yi, Y., Gao, S., Xia, J., Li, C., Zhao, Y., Zhang, Y., Liang, A., Ji, S., 2020. Study of the accumulation and distribution of arsenic species and association with arsenic toxicity in rats after 30 days of oral realgar administration. J. Ethnopharmacol. 247, 111576 https://doi.org/10.1016/j.jep.2018.10.037.